Dynamics of Earth-Orbiting Flexible Satellites with Multibody Components

L. Vu-Quoc* and J. C. Simo†
Stanford University, Stanford, California

A novel approach to the dynamics of satellites with flexible multibody components is proposed. The property of invariance under superposed rigid-body motions of geometrically-exact structural theories is employed to refer the dynamics of motion directly to the *inertial frame*. To avoid numerical ill conditioning, the dynamics of the far field and the near field are treated separately by introducing a *rotationally-fixed floating frame*, which is a parallel translate of the inertial frame. Constraint conditions to determine the orientation of floating frames proposed in the past are thus entirely bypassed. The proposed formulation can accommodate an unrestricted class of maneuvers under the action of follower forces and gravitational force, and is particularly suited for the dynamics of flexible multibody systems undergoing a broad range of deformations.

Introduction

Satellite Dynamics: Floating Frames

FUTURE Earth-orbiting satellites will be of very large size, constructed using lightweight materials, and therefore very flexible.[1] Current approaches to the dynamics of flexible structures in orbit are largely based on the assumption of small deformation, and rely on the use of a floating reference frame to describe the structural displacements. Linearized strain measures are thus employed in these formulations. The floating frames must translate and rotate with the deformed structure such that the structural displacements fall within the range of validity of the small deformation assumption.[2,3]

For the type of highly flexible large space structures described, there is no guarantee that deformations will remain small. Hence, traditional approaches employing the small strain assumption would yield only a first-order approximation of the nonlinear displacement field. In addition, for the case of rotating flexible structures, we have shown in Ref. 4 that employing linearized strain measures can lead to grossly inaccurate results. On the other hand, our methodology represents a departure from the traditional approaches in that, by employing *geometrically-exact structural theories*, which are invariant with respect to superposed rigid-body motions, *the dynamics of the structure is directly referred to the inertial frame*. Thus, we completely bypass the use of a (rotating) floating reference frame. Moreover, by referring the dynamics to the inertial frame, the inertia terms in the equations of motion are much simpler as compared with those resulting from the use of a *rotating* floating frame: The coupling and nonlinearity, because of the presence of centrifugal force, Coriolis force, and inertia force due to rotation, are consequently eliminated. Within the proposed framework, inertia terms in the equations of motion have a structure identical to that found in rigid-body mechanics. The reader is referred to Refs. 5–7 and 18 for several aspects of the proposed approach.

For a flexible satellite, however, since structural deformations are extremely small compared to the distance separating the center of the Earth and satellite, numerical ill conditioning would result if the dynamics of the satellite were referred directly to the inertial frame. To avoid this numerical ill conditioning, we propose to express the dynamics of flexible satellites relative to *a parallel translate of the inertial frame*, whose origin is placed at the instantaneous center of mass of the satellite. We emphasize here that, unlike previously employed floating frames[2] which actually rotate with the deformed structures, *the proposed floating frame does not rotate with respect to the inertial frame*. The procedure to integrate the resulting equations of motion is discussed in detail. Further, the action of configuration-dependent actuator forces can be conveniently accounted for within the formulation.[7–9]

Multibody Dynamics

There exists a vast body of literature on multibody dynamics starting with the pioneering work by Hooker and Margulies[11] and Roberson and Wittenburg.[12] Although most of the research in this area is focused on systems of rigid bodies, attention has been directed recently to the study of flexible multibody systems. Jerkowsky gives an overview of several approaches to the dynamics of n-body systems in Ref. 13. An extensive reference list is contained in Ref. 14. Ho and Herber[15] classify multibody systems into six categories in the order of increasing difficulty in the formulation. This classification contains the all-flexible chain systems and the all-flexible topological tree multibody systems as the two most difficult classes of problems, but excludes flexible closed loops. (That is, a set of $(n+1)$ bodies interconnected by n points; each of these points is common to two bodies. The tree topology thus implies the absence of closed loops.) Treatment of the flexible chain system may be found for example in Ref. 16, while treatment of the more complex topological tree multibody system is explored in Ref. 14. In general, with the presence of closed loops, additional nonholonomic constraints have to be included in the equations of motion,[17] and thus require special care in the numerical integration procedure.

As a direct by-product of our formulation, one could easily treat the above-mentioned classes of problems, including closed loops. This is achieved without any alteration in the formulation and without any additional constraints, since hinge conditions are accounted for in a straightforward manner using the Galerkin finite-element discretization of the spatial variable in the equations of motion. Reference 6 contains several examples that involve flexible chains undergoing large overall motions. Further, there is no limitation imposed on the range of structural deformation or the speed of evolution of the system. An example of a very flexible closed-loop chain is given herein. Although the proposed methodology is applica-

Received March 17, 1986; revision received March 5, 1987.

*Postdoctoral Research Fellow, Applied Mechanics Division.
†Assistant Professor, Applied Mechanics Division.

ble to a large class of structural elements—beams, plates, shells, 3-D continua—we shall limit our discussion to the case of a flexible satellite composed of beam elements.

Geometrically-Exact Beam Model: Equations of Motion

Basic Kinematic Description

Let $\{O; \boldsymbol{e}_1, \boldsymbol{e}_2, \boldsymbol{e}_3\}$ represent the inertial frame with origin O and the orthonormal basis vectors $\{\boldsymbol{e}_1, \boldsymbol{e}_2, \boldsymbol{e}_3\}$. Consider a beam of length L initially straight and arbitrarily positioned in the three-dimensional space. Let S denote the coordinate along the line of centroids of the beam: $0 \le S \le L$. A plane cross section Ω of the beam, initially perpendicular to the line of centroids, is assumed to remain plane after deformation, but needs not be perpendicular to the deformed line of centroids. Thus, we account for shear deformation in this formulation.

Let $\{\boldsymbol{t}_1, \boldsymbol{t}_2, \boldsymbol{t}_3\}$ denote the orthonormal basis vectors attached to a typical cross section with the origin placed at the centroid, and such that $\{\boldsymbol{t}_1, \boldsymbol{t}_2\}$ lie in the plane of the cross section and $\boldsymbol{t}_3$ is normal to the cross section at all times. The orthogonal transformation from the inertial basis $\{\boldsymbol{e}_i\}$ to the cross-section basis $\{\boldsymbol{t}_i(S,t)\}$ is represented by the orthogonal matrix $\Lambda(S,t)$, where t denotes the time parameter. In component form, we have $\boldsymbol{t}_i(S,t) = \Lambda_{ij}(S,t)\boldsymbol{e}_j$,[‡] where Λ_{ij} designates the "(i,j)" coefficient of matrix Λ.

The position vector of the centroid of a cross section with respect to origin O is represented by $\phi_0(S,t) = S\boldsymbol{t}_3(S,0) + \boldsymbol{u}(S,t)$, where $\boldsymbol{u} = u_i\boldsymbol{e}_i$ denotes the displacement vector of the centroid. The deformation of the beam can thus be described by the motion of a typical cross section: 1) the position of the centroid as given by the vector $\phi_0(S,t) = \phi_{0i}(S,t)\boldsymbol{e}_i$, and 2) the orientation of the cross section as given by the orthogonal matrix $\Lambda(S,t)$.

Equations of Motion

We denote by $\overset{\vee}{\boldsymbol{\theta}}$ the skew-symmetric matrix associated with the vector $\boldsymbol{\theta} = \theta_i\boldsymbol{e}_i$, such that

$$\overset{\vee}{\boldsymbol{\theta}} = \begin{bmatrix} 0 & -\theta_3 & \theta_2 \\ \theta_3 & 0 & -\theta_1 \\ -\theta_2 & \theta_1 & 0 \end{bmatrix}. \tag{1}$$

The complete set of equations of motion of the free-free beam is summarized in Table 1, where $\boldsymbol{n} = n_i\boldsymbol{e}_i$ and $\boldsymbol{m} = m_i\boldsymbol{e}_i$ represent, respectively, the internal force and the internal moment acting on a typical cross section of the beam; $\bar{\boldsymbol{n}}$ and $\bar{\boldsymbol{m}}$ denote the distributed applied force and moment.

The function $\Psi(S,\Gamma,\Omega)$ corresponds to the constitutive law relating the strain measure Γ and curvature Ω to the internal force $\boldsymbol{n}$ and moment $\boldsymbol{m}$. We often assume in practice that Ψ takes a quadratic form

$$\Psi(S,\Gamma,\Omega) := \frac{1}{2}\begin{Bmatrix}\Gamma\\ \Omega\end{Bmatrix}^T \boldsymbol{C}\begin{Bmatrix}\Gamma\\ \Omega\end{Bmatrix}, \tag{2}$$

$$\boldsymbol{C} := \mathrm{diag}[GA_1, GA_2, EA, EI_1, EI_2, GJ], \tag{3}$$

where GA_1 and GA_2 denote, respectively, the shear stiffnesses along the axes $\boldsymbol{t}_1$ and $\boldsymbol{t}_2$, EA is the axial stiffness along $\boldsymbol{t}_3$, EI_1 and EI_2 are the principal bending stiffnesses relative to axes $\boldsymbol{t}_1$ and $\boldsymbol{t}_2$, respectively, and GJ is the Saint Venant torsional stiffness along $\boldsymbol{t}_3$.

In Table 1, $A_\rho := \int_\Omega \rho_0 \mathrm{d}\Omega$ with ρ_0 the mass density, represents the mass per unit length of the beam, and $\mathbf{I}_\rho(S,t)$ the mass inertia dyadic of the cross section relative to the inertial basis $\{\boldsymbol{e}_i\}$. Let $\mathbf{\Pi}_\rho(S)$ denote the mass inertia dyadic of the cross section relative to the cross-section basis $\{\boldsymbol{t}_i\}$. We then have

$$\mathbf{\Pi}_\rho(S) = \Lambda^T(S,t)\mathbf{I}_\rho(S,t)\Lambda(S,t). \tag{4}$$

Note that the inertia terms in the equations of balance of linear and angular momenta in Table 1 are those of a cross section viewed as a rigid body. The reader is referred to Refs. 7–9 and 18 for further explanation of the formulation and for the detailed numerical treatment of the equations in Table 1.

Table 1 Equations of motion of a free-free geometrically-exact beam

$$\frac{\partial\Lambda(S,t)}{\partial S} = \overset{\vee}{\boldsymbol{\omega}}(S,t)\Lambda(S,t), \quad \frac{\partial\Lambda(S,t)}{\partial t} = \overset{\vee}{\boldsymbol{w}}(S,t)\Lambda(S,t)$$

$$\Gamma = \Lambda^T(S,t)\frac{\partial\phi_0(S,t)}{\partial S} - \Lambda^T(S,0)\frac{\partial\phi_0(S,0)}{\partial S}, \quad \Omega = \Lambda^T\omega$$

$$\boldsymbol{n} = \Lambda\frac{\partial\Psi(S,\Gamma,\Omega)}{\partial\Gamma}, \quad \boldsymbol{m} = \Lambda\frac{\partial\Psi(S,\Gamma,\Omega)}{\partial\Omega}$$

$$\frac{\partial\boldsymbol{n}}{\partial S} + \bar{\boldsymbol{n}} = A_\rho\ddot{\phi}_0$$

$$\frac{\partial\boldsymbol{m}}{\partial S} + \frac{\partial\phi_0}{\partial S}\times\boldsymbol{n} + \bar{\boldsymbol{m}} = \mathbf{I}_\rho\dot{\boldsymbol{w}} + \boldsymbol{w}\times[\mathbf{I}_\rho\boldsymbol{w}]$$

$$\boldsymbol{n}(0,t) = \boldsymbol{n}(L,t) = 0$$

$$\boldsymbol{m}(0,t) = \boldsymbol{m}(L,t) = 0$$

Dynamics of Flexible Satellites

Mathematically, the system of partial differential equations summarized in Table 1 completely describes the dynamics of a flexible satellite constituted of beam elements: the Earth gravitation enters as distributed applied force $\bar{\boldsymbol{n}}$. However, using finite-precision mathematics for computation, such formulation becomes numerically ill-conditioned when the dynamics is referred directly to the inertial frame. The reason for this ill conditioning becomes clear when comparing the magnitude of structural deformations with the distance from the satellite to the center of the Earth. In this section, we present a method to remedy this shortcoming.

Rotationally-Fixed Floating Frame

We introduce the frame $\{Z; \boldsymbol{a}_1, \boldsymbol{a}_2, \boldsymbol{a}_3\}$, as shown in Fig. 1, with origin Z whose position relative to origin O of the inertial frame is given by the position vector $\boldsymbol{Z}(t) = Z_i(t)\boldsymbol{e}_i$, and such that the orthonormal basis vectors $\{\boldsymbol{a}_i\}$ have constant components relative to the inertial basis $\{\boldsymbol{e}_i\}$. Thus, this floating frame only translates, but does not rotate with respect to the inertial frame; hence, the name of *rotationally-fixed*

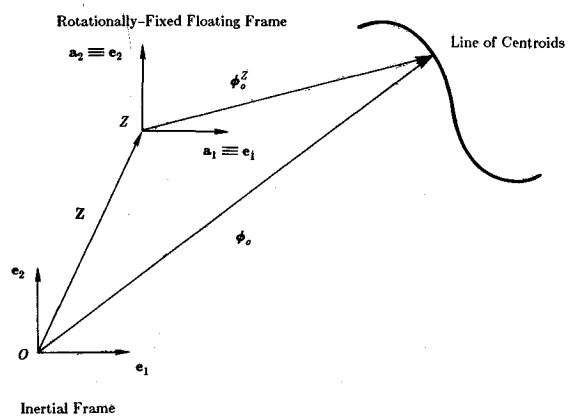

Fig. 1 Rotationally-fixed floating frame: Parallel translate of the inertial frame.

[‡]Summation convention is implied on repeated indices. These indices take values in $\{1,2,3\}$.

floating frame. For convenience, we choose $a_k \equiv e_k$, which makes $\{Z; e_1, e_2, e_3\}$ simply a parallel translate of the inertial frame $\{O; e_1, e_2, e_3\}$. Let $\phi_0^Z(S,t) = \phi_{0i}^Z(S,t)e_i$ denote the position vector of the line of centroids of the beam relative to origin Z. Then

$$\phi_0(S,t) = Z(t) + \phi_0^Z(S,t) = \left[Z_i(t) + \phi_{0i}^Z(S,t)\right] e_i. \quad (5)$$

We refer to the map $t \to Z(t)$ as the *far-field* dynamics, which will be used later to describe the position of the satellite relative to the inertial frame. By the dynamics of the *near field*, we refer to the map $t \to \phi_0^Z(S,t)$, which describes the structural deformation.

Loading Conditions

Three types of loading are considered. The simplest one is the spatially-fixed loading with (possibly time varying) components relative to the inertial basis vectors as given by $\bar{n}^f(t) = n_i^f(t)e_i$. Most relevant to flexible satellites is the loading that follows the structural deformation, such as the actuator control force—coming, for example, from gas jets or ion thrusters —used for the pointing maneuver and vibration suppression. The actuator control force considered herein falls into the category of *follower loading* of the circulatory type, i.e., loading that is not derivable from a potential and not explicitly dependent on time, defined as follows:

$$\bar{n}^a(t) := N_i^a(t)t_i(t) = \Lambda_{ij}(S,t)N_j^a(t)e_j. \quad (6)$$

The applied load in Eq. (6) thus follows the change in orientation of the cross section, represented by the basis $\{t_i\}$, and may have time-varying magnitude. Since the follower load $\bar{n}^a$ is explicitly dependent on Λ, we will often write $\bar{n}^a(\Lambda)$. Finally, gravity loading derived from spherical potential applied to a material point of mass A_ρ located at a distance ϕ_0 from the source, here the origin O, of the form

$$\bar{n}^g(\phi_0) = -\frac{A_\rho \mu \phi_0}{\|\phi_0\|^3}, \quad (7)$$

with μ denoting the gravitational constant, is also configuration dependent. Using Eq. (7) in the preceding beam model implies the reasonable assumption that the mass of the beam is concentrated on the line of centroids. Although more complex models of the gravitation field could be considered,[25,26] our purpose here is only to show how the formulation could accommodate configuration-dependent loading. Hence, within the scope of this paper, we shall consider only the following type of loading:

$$\bar{n} = \bar{n}^f + \bar{n}^a(\Lambda) + \bar{n}^g(\phi_0). \quad (8)$$

Far-Field Dynamics

It is essential to note that, in our formulation, the motion of the rotationally-fixed floating frame relative to the satellite, in strict mathematical consideration, *has absolutely no influence* on the mechanical behavior of the satellite. The role of this floating frame can be thought of simply as a "zooming device," and serves the sole practical purpose of avoiding numerical ill conditioning resulting from the large difference in magnitude between the structural deformation and the distance from the satellite to the center of the Earth.

Thus, one is free to prescribe the motion of this rotationally-fixed floating frame, provided that it remains within a close neighborhood of the satellite. We choose the following differential equation to describe the motion of the rotationally-fixed floating frame, i.e., the dynamics of the far field,

$$\ddot{Z}(t) = f(Z,\Lambda) := \frac{\mu p}{\|Z\|^2} + \frac{1}{M}\int_{[0,L]} \left[\bar{n}^f + \bar{n}^a(\Lambda)\right] dS, \quad (9)$$

with appropriate initial conditions, where $p := Z/\|Z\|$ is a unit vector, and $M := \int_{[0,L]} A_\rho(S)dS$ the total mass of the satellite. The first term on the right-hand side of Eq. (9) gives the acceleration due to the gravitational field acting on a point mass, whereas the second term represents the acceleration produced by the spatially-fixed force and the follower actuator forces applied on the satellite. We note that Eq. (9), in fact, describes the orbital motion of the instantaneous center of mass of a flexible satellite.

Near-Field Dynamics

In treating the dynamics of the near field, one can always assume that the far field $t \to Z(t)$ is known a priori. As noted previously, the dynamics of a satellite is not affected by the motion of the rotationally-fixed floating frame. Noting that $\partial\phi_0/\partial S \equiv \partial\phi_0^Z/\partial S$ and using the decomposition in Eq. (5), we obtain

$$\frac{\partial n}{\partial S} + \left[\bar{n}^f + \bar{n}^a(\Lambda) + \bar{n}^g\left(Z, \phi_0^Z\right) - A_\rho \ddot{Z}\right] = A_\rho \ddot{\phi}_0^Z,$$

$$\frac{\partial m}{\partial S} + \frac{\partial \phi_0^Z}{\partial S} \times n + \bar{m} = I_\rho \dot{w} + w \times \left[I_\rho w\right]. \quad (10)$$

The strain measure Γ is now evaluated by

$$\Gamma(S,t) = \Lambda^T(S,t)\frac{\partial \phi_0^Z(S,t)}{\partial S} - \Lambda(S,0)^T \frac{\partial \phi_0^Z(S,0)}{\partial S}. \quad (11)$$

It is noted that Eqs. (10) and (11) are the only equations in Table 1 that are modified by the introduction of the decomposition [Eq. (5)].

In all applications of interest, the origin Z of the rotationally-fixed floating frame is located in a small neighborhood of the center of mass. In this case, we have $\epsilon := \|\phi_0^Z\|/\|Z\| \ll 1$. To avoid numerical ill conditioning in the evaluation of the gravitational force $\bar{n}^g(Z, \phi_0^Z)$, one employs the following standard Taylor series expansion, retaining terms up to order $\mathcal{O}(\epsilon^2)$:

$$\bar{n}^g\left(Z, \phi_0^Z\right) \equiv -A_\rho \mu \frac{Z + \phi_0^Z}{\|Z + \phi_0^Z\|^3} = -\frac{A_\rho \mu \phi_0^Z}{\|Z\|^3}\left[1 - \frac{3p \cdot \phi_0^Z}{\|Z\|}\right]$$

$$-\frac{A_\rho \mu p}{\|Z\|^2}\left[1 - \frac{3p \cdot \phi_0^Z}{\|Z\|} - \frac{3}{2}\frac{\|\phi_0^Z\|^2}{\|Z\|^2}\right.$$

$$\left. + \frac{15}{2}\frac{\left(Z \cdot \phi_0^Z\right)^2}{\|Z\|^4}\right] + \mathcal{O}(\epsilon^3). \quad (12)$$

Remark 1. It should be noted that the far-field and near-field dynamics are coupled through the dependence on Λ of the follower actuator force $\bar{n}^a(\Lambda)$ in Eq. (9), and through the presence of the forcing term $A_\rho \ddot{Z}$ as well as the gravity force $\bar{n}^g(Z, \phi_0^Z)$, which depends on the far field $Z(t)$, in Eq. (10).

Dynamic Weak Form of the Near Field

The weak formulation of Eq. (10) governing the dynamics of the near field is the cornerstone of the finite-element solution procedure discussed in the next section. The configuration of a flexible satellite is defined by the functions $\phi_0(S,t) = Z(t) + \phi_0^Z(S,t)$ and $\Lambda(S,t)$. We denote by $\eta(S) := (\eta_0(S), \psi(S))$ an *admissible variation* of the configuration $\phi := (\phi_0^Z, \Lambda)$. Physically, $\eta_0(S) = \eta_{0i}(S)e_i$ represents a superposed infinitesimal displacement field, and $\psi(S) = \psi_i(S)e_i$ a superposed infinitesimal rotation field onto the structure. The (dynamic) weak form of Eq. (10) is obtained by forming the scalar product between Eq. (10) and $\eta(S)$, and by integrating the scalar product over the interval $[0, L]$. After integration by

parts of the resulting expression, there results

$$G_{\text{dyn}}(\phi,\eta) := \int_{[0,L]} \Big\{ A_\rho \ddot{\phi}_0^Z \cdot \eta_0 + \big[\mathbf{I}_\rho \dot{w} + w \times (\mathbf{I}_\rho w)\big] \cdot \psi \Big\} \, dS - G(\phi,\eta), \quad (13)$$

where $G(\phi,\eta)$ denotes the static weak form given by

$$G(\phi,\eta) := \int_{[0,L]} \left\{ n \cdot \left[\frac{\partial \eta_0}{\partial S} - \psi \times \frac{\partial \phi_0^Z}{\partial S} \right] + m \cdot \frac{\partial \psi}{\partial S} \right\} dS - \bar{G}(\phi,\eta), \quad (14)$$

and $\bar{G}(\phi,\eta)$ the weak form of the externally applied loading,

$$\bar{G}(\phi,\eta) := \int_{[0,L]} \Big\{ \big[\bar{n}^f + \bar{n}^g(Z,\phi_0^Z) + \bar{n}^a(\Lambda) - A_\rho \ddot{Z} \big] \cdot \eta_0 + \bar{m} \cdot \psi \Big\} \, dS. \quad (15)$$

It is noted that, in Eq. (15), the far field $Z(t)$ is assumed to be known, and the acceleration term $A_\rho \ddot{Z}$ is regarded as an additional forcing term.

Computational Solution Strategy

Conceptually, we have to solve for the unknown functions $Z(t)$, $\phi_0^Z(S,t)$, and $\Lambda(S,t)$, such that $\ddot{Z} = f(Z,\Lambda)$ and $G_{\text{dyn}}(\phi,\eta) = 0$ for any admissible η, where $\phi := (\phi_0, \Lambda)$ and $\phi_0 = Z + \phi_0^Z$. We propose a single-step explicit/implicit transient algorithm to solve the preceding coupled far-field/near-field satellite dynamics problem. Consider the time interval of interest $[0,T]$ to be discretized into subintervals such that $[0,T] = \cup_{n \geq 0} [t_n, t_{n+1}]$, where $t_{n+1} = t_n + h$, and h denotes the time step size. Recall that, in a single-step solution procedure, the solution at time t_{n+1} is computed based only on the known solution at time t_n.

In line with standard usage, we employ the subscript n to denote the temporal discrete approximate of a time-varying quantity at time t_n; thus, for the far field, $Z_n \cong Z(t_n)$; for the near field, $d_n(S) \cong \phi_0^Z(S,t_n)$, $v_n(S) \cong \dot{\phi}_0^Z(S,t_n)$, and $a_n(S) \cong \ddot{\phi}_0^Z(S,t_n)$; and for the rotation field, $\Lambda_n(S) \cong \Lambda(S,t_n)$, $w_n(S) \cong w(S,t_n)$, and $\alpha_n(S) \cong \dot{w}(S,t_n)$. Also denote the configuration at time t_n as $\phi_n(S) := (d_n(S), \Lambda_n(S))$.

Far-Field Dynamics: Explicit Scheme

The ordinary differential equation (ode) (1) describing the motion of the origin Z of the rotationally-fixed floating frame is easily solved by employing any of the classical explicit single-step algorithms for ode's (e.g., see Refs. 19 and 20) when the function $f(Z,\Lambda)$ is explicitly known. However, the function $\Lambda(S,t)$ for $t \geq t_n$ is not known until the equations of motion (10) have been solved. Hence, to solve for Z_{n+1}, using the known solution $\{Z_n, \Lambda_n(S)\}$, we assume that $\Lambda(S,t) \equiv \Lambda_n(S)$, for all $t \in [t_n, t_{n+1}]$. This assumption implies that the follower load is constant in the interval $[t_n, t_{n+1}]$. In the implementation, we employ the explicit Runge-Kutta fourth-order method.

Remark 2. A wide choice of numerical algorithms for ode's—explicit or implicit, single step or multistep—could be used to solve for the far field with the preceding assumption. In general, due to structural vibration, the time step size of the whole numerical integration scheme is governed by the near-field dynamics.

Remark 3. Numerical integration of the far-field dynamics is only necessary when external forces from other than the gravitational field are applied on the satellite. In the absence of these applied forces, one can use well-known analytical solutions in orbital mechanics (the two-body problem) to obtain directly the solution for the far field $Z(t)$.

Remark 4. Because of the assumption that the follower load remains constant in the interval $[t_n, t_{n+1}]$ for the integration of the far field, the origin Z of the rotationally-fixed floating frame will not follow the path of the center of mass of the satellite exactly, and could gradually drift away from the latter. We note that the assumption of piecewise constant applied follower loading used in the integration of the far field is closely related to the rectangular integration rule. This assumption can be viewed as a convenient interpolation of the follower actuator load; the role of this interpolation is to allow a decoupling in the numerical treatment of the coupled far-field/near-field problem. However, due to the small time step size to accommodate structural vibration, the drift of origin Z from the center of mass would be insignificant. In addition, since one could always arbitrarily reposition the floating frame relative to the satellite, as will be shown later, the drift of origin Z from the center of mass is therefore inconsequential as far as the structural response of the satellite is concerned.

Near-Field Dynamics: Implicit Scheme

The basic problem concerning the discrete time-stepping algorithm for the near field may be formulated as follows. With Z_{n+1} known from solving the far-field dynamics as described previously, and given the known configuration $\phi_n := (d_n, \Lambda_n)$ at time t_n, its associated linear and angular velocities (v_n, w_n), and linear and angular accelerations (a_n, α_n), we want to obtain the configuration $\phi_{n+1} := (d_{n+1}, \Lambda_{n+1})$ at time t_{n+1}, the associated linear and angular velocities (v_{n+1}, w_{n+1}), and the linear and angular acceleration (a_{n+1}, α_{n+1}) in a manner that is *consistent* and *stable* with the dynamic weak form $G_{\text{dyn}}(\phi,\eta) = 0$, for all admissible variation η.

To this end, we propose the generalized implicit Newmark algorithm summarized in Table 2. Note that the algorithm for the translational part of the configuration, i.e., $\phi_0^Z(S,t)$, is the classical Newmark algorithm of nonlinear elastodynamics.[10,21] The proposed algorithm for the rotational part, i.e., $\Lambda(S,t)$, furnishes the canonical extension of the Newmark formulas to the group of orthogonal matrices describing the rotation field of the beam. Recall that the rotation matrix corresponding to a rotation vector θ is given by[22,23]

$$\exp[\overset{\vee}{\theta}] := \sum_{k \geq 0} \frac{[\overset{\vee}{\theta}]^k}{k!} = \mathbf{1}_3 + \frac{\sin\|\theta\|}{\|\theta\|} \overset{\vee}{\theta} + 1/2 \frac{\sin^2(\|\theta\|/2)}{(\|\theta\|/2)^2} \overset{\vee}{\theta}^2 \quad (16)$$

in which $\mathbf{1}_k$ denotes the unit $k \times k$ matrix. In Table 2, β and τ are the parameters in the Newmark algorithm, which re-

Table 2 Generalized implicit Newmark algorithm

Momentum balance at t_{n+1} $G_{\text{dyn}}(\phi_{n+1},\eta) = 0$, for all η admissible	
Translation	Rotation
$d_{n+1} := d_n + u_n$	$\Lambda_{n+1} := \Lambda_n \exp[\Lambda_n^T \overset{\vee}{\theta}_n \Lambda_n]$
$u_n := hv_n + h^2[(1/2-\beta)a_n + \beta a_{n+1}]$	$\theta_n := hw_n + h^2[(1/2-\beta)\alpha_n + \beta\alpha_{n+1}]$
$v_{n+1} := v_n + h[(1-\tau)a_n + \tau a_{n+1}]$	$w_{n+1} := w_n + h[(1-\tau)\alpha_n + \tau\alpha_{n+1}]$

duces to the trapezoidal rule when $\beta = \frac{1}{4}$ and $\tau = \frac{1}{2}$. Detailed discussion of the preceding algorithm is lengthy and is not within the scope of the present paper. We refer to Ref. 7 and Ref. 9 for a geometric interpretation, the error analysis, as well as the incremental form of this algorithm.

Remark 5. The accuracy of the implicit integration scheme for the near field is independent of the accuracy of the integration scheme for the far field in the sense that we always obtain the structural displacement and rotation of the beam up to second-order accuracy,[7] regardless of the choice of integration scheme for the far field.

Linearization: Tangent Operators

We recall that, as a result of introducing the generalized Newmark time-stepping algorithm outlined in Table 2, the weak form $G_{\text{dyn}}(\phi_{n+1}, \eta) = 0$ governing the dynamics of the near field becomes a nonlinear functional depending on the unknown $\phi_{n+1}(S) := (\boldsymbol{d}_{n+1}(S), \Lambda_{n+1}(S))$. In what follows, we will be concerned with the spatial discretization of this nonlinear functional by a Galerkin procedure. First, we provide some detail concerning the linearization of the loading term involving the gravitational force.

The solution of the nonlinear variational problem $G_{\text{dyn}}(\phi_{n+1}, \eta) = 0$ by Newton's method involves the solution of a sequence of linearized problems, denoted by $L[G(\phi_{n+1}^{(i)}, \eta)] = 0$, where the superscript i designates the iteration number. These linear problems are obtained by a consistent linearization of $G_{\text{dyn}}(\phi, \eta) = 0$ at the configuration $\phi \equiv \phi_{n+1}^{(i)}(S)$ in the direction of the incremental displacement and rotation $\Delta\phi_{n+1}^{(i)}(S) := (\Delta \boldsymbol{u}_{n+1}^{(i)}(S), \Delta\theta_{n+1}^{(i)}(S))$ according to

$$L\left[G_{\text{dyn}}\left(\phi_{n+1}^{(i)}, \eta\right)\right] = G_{\text{dyn}}\left(\phi_{n+1}^{(i)}, \eta\right) + DG_{\text{dyn}}\left(\phi_{n+1}^{(i)}, \eta\right)\Delta\phi_{n+1}^{(i)} = 0. \quad (17)$$

The second term in Eq. (17) is linear with respect to $\Delta\phi_{n+1}^{(i)}$, and can be evaluated employing the directional derivative formula [the superscript i and the subscript $n+1$ have been deleted in Eq. (18) to alleviate the notation]:

$$DG_{\text{dyn}}(\phi, \eta)\Delta\phi = \frac{\mathrm{d}}{\mathrm{d}\epsilon}\Big|_{\epsilon=0} G_{\text{dyn}}(\phi_\epsilon, \eta), \quad (18)$$

where $\phi_\epsilon = (\boldsymbol{d}_\epsilon, \Lambda_\epsilon)$ denotes the perturbed configuration defined as follows[7,8]:

$$\boldsymbol{d}_\epsilon := \boldsymbol{d} + \epsilon\Delta\boldsymbol{u}, \quad \Lambda_\epsilon := \exp\left[\epsilon\Delta\overset{\vee}{\theta}\right]\Lambda. \quad (19)$$

A detailed account of the linearization process for the static weak form $G(\phi_{n+1}^{(i)}, \eta)$ defined in Eq. (14) that includes follower loading is contained in Ref. 8. Extension of this methodology to the dynamic problem governed by $G_{\text{dyn}}(\phi_{n+1}^{(i)}, \eta)$ in Eq. (13) is given in Ref. 7. Thus, within the present context, it remains only to address the linearization of the contribution of the gravitational force field to $\bar{G}(\phi_{n+1}^{(i)}, \eta)$ defined by Eq. (15). This contribution will be denoted by $\bar{G}^g(\phi_{n+1}^{(i)}, \eta)$ in what follows. By making use of the Taylor series expansion of Eq. (12) in Eq. (15), application of the directional derivative formula [Eq. (18)] to $\bar{G}^g$ yields the expression

$$D\bar{G}^g\left(\phi_{n+1}^{(i)}, \eta\right)\Delta\phi_{n+1}^{(i)} = -\int_{[0,L]} \frac{A_\rho \mu \eta_0}{\|\boldsymbol{Z}_{n+1}\|^3} \cdot \left[3\left(1 - \frac{5\boldsymbol{p}_{n+1}\cdot\boldsymbol{d}_{n+1}^{(i)}}{\|\boldsymbol{Z}_{n+1}\|}\right)\boldsymbol{p}_{n+1}\otimes\boldsymbol{p}_{n+1} + \frac{3}{\|\boldsymbol{Z}_{n+1}\|}\boldsymbol{p}_{n+1}\otimes\boldsymbol{d}_{n+1}^{(i)} + \left(1 - \frac{3\boldsymbol{p}_{n+1}\cdot\boldsymbol{d}_{n+1}^{(i)}}{\|\boldsymbol{Z}_{n+1}\|}\right)\mathbf{1}_3\right]\Delta\boldsymbol{u}_{n+1}^{(i)}\mathrm{d}S, \quad (20)$$

where $\otimes$ denotes the tensor product defined by $[\boldsymbol{a}\otimes\boldsymbol{b}]\boldsymbol{c} = (\boldsymbol{b}\cdot\boldsymbol{c})\boldsymbol{a}$, with $\boldsymbol{a}$, $\boldsymbol{b}$, and $\boldsymbol{c}$ being arbitrary vectors. If one identifies a vector to a column matrix of its components, then $[\boldsymbol{a}\otimes\boldsymbol{b}] = [\boldsymbol{a}\boldsymbol{b}^T]$. Note that the preceding tangent gravity load stiffness operator is nonsymmetric and involves only the translational degrees of freedom. Equation (20) will be used in the computation of the load stiffness matrix upon introducing the spatial discretization.

Spatial Discretization: Galerkin Finite-Element Method

We begin by introducing a partition of the interval $[0, L]$ into nonoverlapping subintervals according to $[0, L] = \cup_{k=1}^{N-1}[S_k, S_{k+1}]$, where $0 \equiv S_1 < S_2 < \cdots < S_N \equiv L$. Consider the following approximation for the translational field:

$$\boldsymbol{d}_{n+1}(S) \cong \sum_{I=1}^{N} N_I(S)\,\boldsymbol{d}_{n+1,I}, \quad (21)$$

where $\boldsymbol{d}_{n+1,I} \cong \boldsymbol{d}_{n+1}(S_I)$. Here, $N_I(S)$ is a set of global functions that are either prescribed or constructed from local finite-element approximations in the standard manner. An interpolation for $\Lambda_{n+1}(S)$ is constructed by noting that $\Lambda_{n+1}(S) = \exp[\overset{\vee}{\chi}_{n+1}(S)]$, where χ_{n+1} represents the rotation vector associated with Λ_{n+1}. We then consider the approximation for the rotation field

$$\chi_{n+1}(S) \cong \sum_{I=1}^{N} N_I(S)\,\chi_{n+1,I},$$

where

$$\chi_{n+1,I} \cong \chi_{n+1}(S_I) \text{ and } \Lambda_{n+1}(S) = \exp[\overset{\vee}{\chi}_{n+1}(S)]. \quad (22)$$

Note that the approximation scheme [Eq. (22)] preserves exactly the orthogonality property of Λ. Substituting the interpolation in Eqs. (21) and (22) into the linearized weak form [Eq. (17)], and assuming that the incremental displacement field $\Delta\phi_{n+1}^{(i)} := (\Delta\boldsymbol{u}_{n+1}^{(i)}, \Delta\theta_{n+1}^{(i)})$ and the admissible variations $\eta := (\eta_0, \psi)$ are approximated in the same manner according to

$$\Delta\phi_{n+1}^{(i)}(S) \cong \sum_{I=1}^{N} N_I(S)\,\Delta\phi_{n+1,I}^{(i)} \quad (23)$$

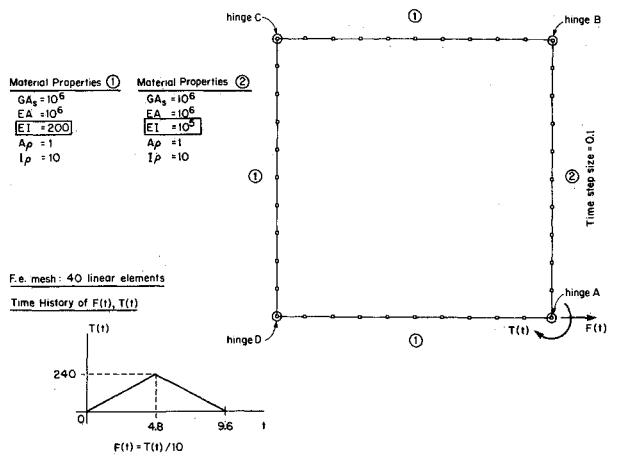

Fig. 2 Flying closed-loop chain. Problem data.

with $\Delta\phi^{(i)}_{n+1,I} \equiv \Delta\phi^{(i)}_{n+1}(S_I)$, and

$$\eta(S) \equiv \sum_{I=1}^{N} N_I(S)\eta_I, \tag{24}$$

with $\eta_I \equiv \eta(S_I)$, we arrive at a system of linear equations

$$P_I\left(\phi^{(i)}_{n+1}\right) + \sum_{J=1}^{N} K_{IJ}\left(\Lambda_n, \phi^{(i)}_{n+1}\right)\Delta\phi^{(i)}_{n+1,J} = O \tag{25}$$

for $I = 1,\ldots, N$. In Eq. (25), P_I represents the residual force, and K_{IJ} the dynamic tangent stiffness matrix obtained from

$$K_{IJ}\left(\Lambda_n, \phi^{(i)}_{n+1}\right) = M_{IJ}\left(\Lambda_n, \Lambda^{(i)}_{n+1}\right) + S_{IJ}\left(\phi^{(i)}_{n+1}\right) + G_{IJ}\left(\phi^{(i)}_{n+1}\right) + L^a_{IJ}\left(\Lambda^{(i)}_{n+1}\right) + L^g_{IJ}\left(Z_{n+1}, d^{(i)}_{n+1}\right). \tag{26}$$

Expressions for the tangent inertia matrix M_{IJ}, the tangent material stiffness matrix S_{IJ}, the tangent geometric stiffness matrix G_{IJ}, and the tangent follower load stiffness L^a_{IJ} have been obtained in Refs. 7 and 8, and are summarized in the Appendix. The expression for the tangent gravity load stiffness results from the introduction of approximation equations (21), (23), and (24) into Eq. (20),

$$L^g_{IJ}\left(Z^i_{n+1}, d^i_{n+1}\right) = -\int_{[0,L]} \frac{A_\rho \mu}{\|Z_{n+1}\|^3} \cdot \left[3\left(1 - \frac{5p_{n+1}\cdot d^{(i)}_{n+1}(S)}{\|Z_{n+1}\|}\right) p_{n+1}\otimes p_{n+1} + \frac{3}{\|Z_{n+1}\|} p_{n+1}\otimes d^{(i)}_{n+1}(S) + \left(1 - \frac{3p_{n+1}\cdot d^{(i)}_{n+1}(S)}{\|Z_{n+1}\|}\right)\mathbf{1}_3\right] N_I(S) N_J(S)\,dS. \tag{27}$$

The incremental displacement and rotation $\Delta\phi^{(i)}_{n+1}$ is computed by solving the linear system [Eq. (25)]. Next, one performs the update according to Eq. (19) to obtain the solution $\phi^{(i+1)}_{n+1}$ at iteration $(i+1)$. The complete update procedure is, however, nontrivial. The reader is referred to Refs. 7–9 for detailed discussions.

Repositioning of the Rotationally Fixed Floating Frame

One of the salient features of our formulation is that the rotationally-fixed floating frame could be arbitrarily repositioned, and its velocity with respect to the inertial frame could be reset at any time. Thus, in case of a drift of the origin Z of the floating frame from the center of mass, one could easily reposition the floating frame to the center of mass by first computing the current position of the instantaneous center of mass relative to Z. This position is denoted by r such that

$$r(t) = \frac{1}{M}\int_{[0,L]} A_\rho(S)\,\phi^Z_0(S,t)\,dS. \tag{28}$$

The velocity and acceleration of the center of mass relative to the floating frame are given by

$$\dot r(t) = \frac{1}{M}\int_{[0,L]} A_\rho(S)\,\dot\phi^Z_0(S,t)\,dS, \tag{29}$$

$$\ddot r(t) = \frac{1}{M}\int_{[0,L]} A_\rho(S)\,\ddot\phi^Z_0(S,t)\,dS. \tag{30}$$

Only when $\|Z\|$ and $\|r\|$ are of comparable magnitude, so that loss of precision on the structural deformation may occur due to round-off error, that the repositioning procedure need be performed. In this case, if we wish to reposition the floating frame at time $t = \bar t$, we simply restart the integration of the far-field dynamics with initial conditions reset as follows:

$$Z(\bar t) \leftarrow [Z(\bar t) + r(\bar t)],$$
$$\dot Z(\bar t) \leftarrow [\dot Z(\bar t) + \dot r(\bar t)]. \tag{31}$$

The near-field dynamics is also reset according to

$$\phi^Z_0(\bar t) \leftarrow [\phi^Z_0(\bar t) - r(\bar t)],$$
$$\dot\phi^Z_0(\bar t) \leftarrow [\dot\phi^Z_0(\bar t) - \dot r(\bar t)],$$
$$\ddot\phi^Z_0(\bar t) \leftarrow [\ddot\phi^Z_0(\bar t) - \ddot r(\bar t)]. \tag{32}$$

It is clear that the preceding repositioning procedure leaves the value at time $\bar t$ of $\phi_0(\bar t) = Z(\bar t) + \phi^Z_0(\bar t)$ strictly unchanged, and hence the values of the velocity $\dot\phi_0(\bar t)$, and of the acceleration $\ddot\phi_0(\bar t)$. Further, this repositioning procedure is most conveniently employed when a single-step integration algorithm for ode's is used to solve for the far field.

Numerical Examples

We now give some numerical examples that involve the dynamics of flexible multibody systems, the concept of a rotationally-fixed floating frame, and the dynamics of Earth-orbiting satellites to illustrate the effectiveness and generality of the proposed formulation. All figures of the deformed shapes reported herein are given at the same scale as the geometry of the structure: There is *no artificial magnification of the structural deformation* for visualization purposes.

Example 1—Flying Closed-Loop Chain

To demonstrate the capability of the present approach to model the dynamics of flexible multibody systems, we consider a closed-loop chain constituted of four flexible links interconnected by hinges as shown in Fig. 2. One of the links is 500 times stiffer than the other three: Link AB in Fig. 2 has

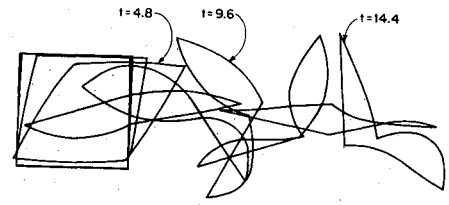

Fig. 3 Flying closed-loop chain. Entire sequence of motion.

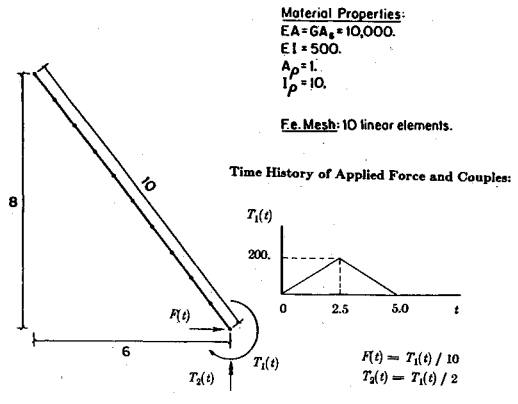

Fig. 4 Flying flexible beam in 3-D motion. Problem data.

a bending stiffness of $EI = 10^5$, while the remaining links have a bending stiffness of $EI = 200$. The other material properties are chosen to be identical for the four links, and are listed in Fig. 2. Initially, the closed-loop chain forms a square of length 10 on each side. The whole system has no prescribed displacement boundary condition. To create the forward motion, a force is applied at end A of the stiff link AB; the overall tumbling motion of the chain is induced by a torque applied at the same end as shown in Fig. 2, together with the time history of their magnitude. Figure 3 depicts the entire sequence of motion. A time step size of $h = 0.1$ is used throughout the analysis.

Example 2—Flying Flexible Beam in 3-D Motion

We consider a free-free flexible beam initially placed at an inclined position and subject to applied force and torques at the lower free end as shown in Fig. 4. This example has been previously analyzed in Ref. 7 using the time-stepping algorithm partly summarized in Table 2, together with the Galerkin finite-element method to solve the system of equations given in Table 1. Our purpose here is to show how the concept of decomposition of the deformation map into the far field and the near field, given in Eq. (5), could be employed in a simple manner. The overall translational motion of the beam results from the applied force along the axis e_1, whereas the forward tumbling motion results from the torque about axis e_3, and the out-of-plane motion from the applied torque about axis e_2. These applied force and torques, of the spatially-fixed type mentioned earlier, induce the beam into a "kayak-rowing" motion shown in Figs. 5 and 6. In these figures, finite deformation in the early tumbling stage is clearly discernible.

Since the gravitational field is not considered in this example, and since only spatially-fixed load is applied on the beam, the dynamics of the far field and the near field are completely decoupled:

$$\ddot{\boldsymbol{Z}} = \frac{1}{M}\int_{[0,\,L]} \tilde{\boldsymbol{n}}^f(S)\,\mathrm{d}S, \tag{33}$$

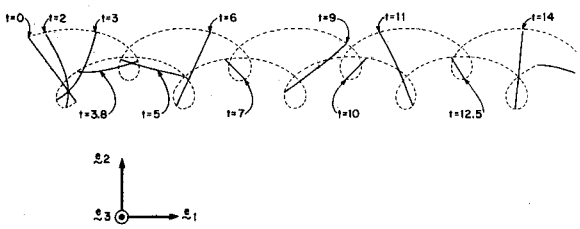

Fig. 5 Flying flexible beam in 3-D motion. Entire sequence of motion projected on plane (e_1, e_2).

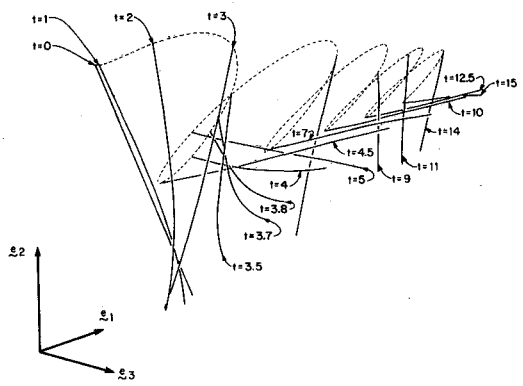

Fig. 6 Flying flexible beam in 3-D motion. Perspective view of entire sequence of motion from an observer fixed in the inertial frame.

$$\frac{\partial \boldsymbol{n}}{\partial S} + \left[\bar{\boldsymbol{n}}^f - A_\rho \ddot{\boldsymbol{Z}}\right] = A_\rho \ddot{\phi}_0^Z. \tag{34}$$

Substitution of Eq. (33) into Eq. (34) yields the equation of motion for the near field

$$\frac{\partial \boldsymbol{n}}{\partial S} + \left[\bar{\boldsymbol{n}}^f - \frac{A_\rho}{M}\int_{[0,\,L]} \bar{\boldsymbol{n}}^f(S)\,\mathrm{d}S\right] = A_\rho \ddot{\phi}_0^Z. \tag{35}$$

Thus, in this example, one does not need to solve for the far field, if only the near-field dynamics is of prime interest. The result of solving for the dynamics of the near field using Eq. (35) instead of Eq. $(10)_1$ is shown in Fig. 7 with a clear physical meaning: The motion given in Fig. 6 as perceived by an inertial observer is now seen by an observer attached to the rotationally-fixed floating frame and moving with the instantaneous center of mass of the beam. A time step size of $h = 0.1$ is used in both analyses (with and without the rotationally-fixed floating frame). A justification of the time step size chosen can be found in Ref. 7.

Example 3—Satellite Dynamics: Libration and Orbit Transfer

Example 1 demonstrates how systems with flexible components connected through hinges can be analyzed with no extra effort in accounting for the hinge constraints that arise in traditional approaches to multibody dynamics. While the analysis of the closed-loop chain in example 1 is performed for the plane motion, our formulation can accommodate fully three-dimensional motion of the beam subjected to a possible state of finite deformation as shown in example 2. The latter example also serves to illustrate the effectiveness of the concept of the rotationally-fixed floating frame. Both these examples, on the other hand, do not take into account the effect of gravitational load.

To illustrate the proposed methodology for solving the coupled far-field/near-field problem in the presence of gravitational force, we consider, in this last example, a beam of length $100\sqrt{2}$ completely contained in the plane $\{e_1, e_2\}$ and placed at 45 deg with respect to axis e_1. The center of mass of the beam is initially located at a distance of 7×10^6 from the center of the Earth (the origin O): $\boldsymbol{Z}(0) = 7 \times 10^6\ e_1$. For the center of mass to describe a circular orbit, an initial velocity of $\dot{\boldsymbol{Z}} = 7544.1557\ e_2$ is chosen; the gravitational constant being $\mu = 3.984 \times 10^{14}$. We are interested in capturing the librational motion resulting from the effect of gravity gradient on orbiting satellites whose geometry departs from spherical symmetry. Hence, for simplicity, we choose the initial condi-

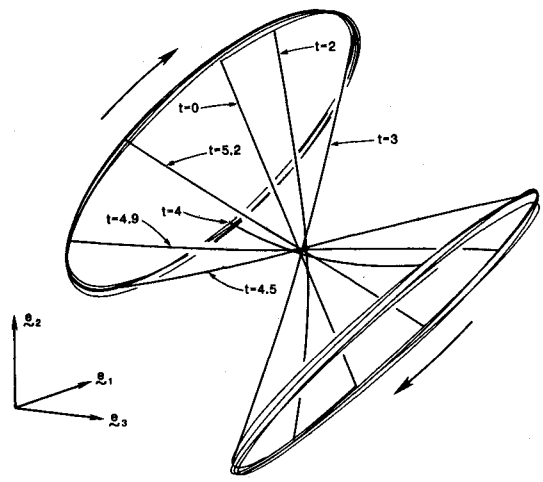

Fig. 7 Flying flexible beam in 3-D motion. Perspective view of entire sequence of motion from an observer fixed in the parallel translate of the inertial frame.

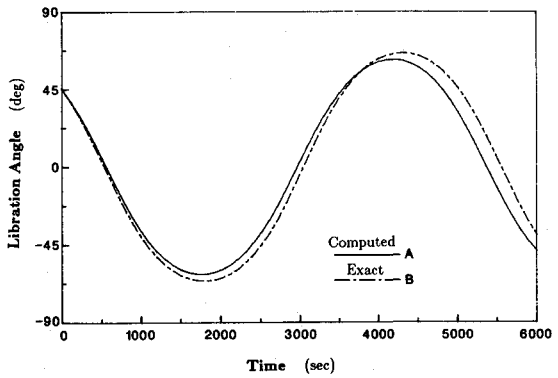

Fig. 8 Satellite dynamics: libration and orbit transfer. Evolution of the libration angle λ on lower circular orbit.

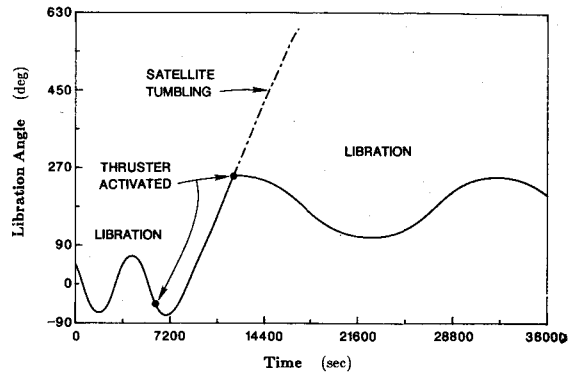

Fig. 10 Satellite dynamics: libration and orbit transfer. Complete time history of the libration angle.

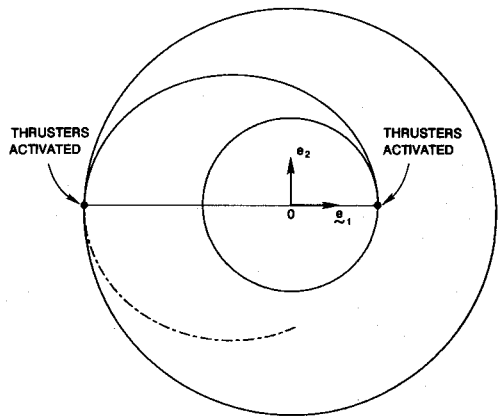

Fig. 9 Satellite dynamics: libration and orbit transfer. Transition from a lower circular orbit to a higher circular orbit.

tions for the near field and for the rotational field to be

$$\phi_0^Z(S,0) = \frac{S - 50\sqrt{2}}{\sqrt{2}}[e_1 + e_2],$$

$$\Lambda(S,0) = \frac{1}{\sqrt{2}}\begin{bmatrix} 1 & -1 & 0 \\ 1 & 1 & 0 \\ 0 & 0 & \sqrt{2} \end{bmatrix}$$

$$\dot{\phi}_0^Z(S,0) = \ddot{\phi}_0^Z(S,0) = w(S,0) = \alpha(S,0) \equiv 0 \qquad (36)$$

Let λ be the (libration) angle between the beam and the unit vector $p := Z/\|Z\|$ known as the local vertical. The dynamics of libration of a uniform bar on circular orbit ($\|Z\| = \text{const}$) is governed by the differential equation[24]

$$\ddot{\lambda} = -\frac{3\mu \sin 2\lambda}{2\|Z\|^3}. \qquad (37)$$

The initial conditions for Eq. (37) that correspond to the preceding chosen initial conditions for the far field and near field are given by $\lambda(0) = \pi/4$ and $\dot{\lambda}(0) = -\|\dot{Z}(0)\|/\|Z(0)\|$. Figure 8 shows the evolution of the libration angle λ obtained using the present approach by solving the far-field/near-field dynamic problem as described previously, and by solving Eq. (37) using the fourth-order explicit Runge-Kutta method. Both curves in Figure 8 are obtained with a time step size of $h = 100$, which, in fact, covers a complete circular orbit in about 60 steps—the orbital period for the preceding initial conditions of the far field is 5830 s. With a smaller time step size, for example, $h = 10$, we can exactly achieve the result as obtained from solving Eq. (37). In addition to the second-order accuracy of the algorithm summarized in Table 2, as compared to the fourth-order accuracy in the integration of Eq. (37), we note that the need for a smaller step size stems from the fact that the semidiscrete equations (ode's) of the equations in Table 1 are indeed much stiffer than Eq. (37).

To demonstrate how a combination of loading given by Eq. (8) could be applied on the satellite, we consider an orbit transfer from the current circular orbit to a higher circular orbit by passing through an intermediate elliptic orbit. This orbit transfer is achieved by activating the satellite thrusters under the form of impulsive loading in two stages. First, when the satellite completes the first revolution in the low circular orbit, impulse loading with resultant in the direction of axis e_2 is applied to induce an increase in magnitude of the velocity $\dot{Z}$, and thus put the satellite into a transitory elliptic orbit as depicted in Fig. 9. The time history of the libration angle (in degrees) is given in Fig. 10. Next, when the satellite reaches the apogee of this transitory orbit, impulsive thruster force, with resultant in the negative direction of axis e_2, is again applied to put the satellite on a higher circular orbit with the radius being the distance from O, the center of the Earth, to the apogee of the elliptic orbit. Since the satellite tumbles on the transitory orbit, as can be seen from Fig. 10, an impulsive moment is also applied at the same time to stop the tumbling and, therefore, subsequently induces the satellite into a librational motion in the higher circular orbit. The radius of the higher orbit is about 1.643×10^7 with an amplitude of libration about 70 deg over one-half of a librational period of about 9610 s. The librational period on this higher orbit can be verified by solving Eq. (37) with appropriate initial conditions. It is emphasized here that Fig. 9 is the plot of computed values of the far field Z, while the plot in Fig. 10 is obtained from the computed values of the near field ϕ_0^Z.

Conclusion

A new approach to the dynamic analysis of flexible Earth-orbiting flexible satellites with multibody components has been presented. The formulation relies essentially on the property of invariance with respect to superposed rigid-body motions of geometrically-exact structural theories. This property leads to considerable simplification of the inertia operator in the equations of motion, as the dynamics of motion is referred to the inertial frame. For satellite dynamics with gravitational loading considered, this property further allows an additive decomposition of the displacement field into the far and near fields. As a consequence, the concept of a rotationally-fixed floating frame is introduced. An efficient integration procedure is then proposed to integrate the coupled far-field/near-field dynamics. The present formulation accounts for the action of follower actuator forces, a type of configuration-dependent loading of particular interest in satellite dynamics. The dynamics of multibody systems composed of flexible

structures interconnected through hinges constitutes a class of problems solvable by the proposed methodology. Finally, we recall that large deformations in the structures are automatically accounted for in the present formulation, and there is absolutely no restriction on the speed of evolution of the systems: all physically relevant phenomena are properly represented.

Appendix: Finite-Element Matrices

We summarize in this appendix the expressions for the tangent matrices that appeared in Eqs. (25) and (26).

Residual Force

$$P_I\left(\phi_{n+1}^{(i)}\right) = \int_{[0,L]} [N_I(S)\mathbf{1}_6] \begin{Bmatrix} A_\rho a_{n+1}^{(i)} \\ \mathbf{I}_{\rho,n+1}^{(i)} \alpha_{n+1}^{(i)} + w_{n+1}^{(i)} \times \left[\mathbf{I}_{\rho,n+1}^{(i)}\right] \end{Bmatrix} dS + \int_{[0,L]} \left[\left\{ \Xi\left(\phi_{n+1}^{(i)}\right)[N_I(S)\mathbf{1}_6] \right\}^T \begin{Bmatrix} n_{n+1}^{(i)} \\ m_{n+1}^{(i)} \end{Bmatrix} - [N_I(S)\mathbf{1}_6] \begin{Bmatrix} \bar{n}(t_{n+1}) \\ \bar{m}(t_{n+1}) \end{Bmatrix} \right] dS, \quad \text{(A1)}$$

where the differential operator Ξ is defined as

$$\Xi(\phi) := \begin{bmatrix} \frac{d}{dS}\mathbf{1}_3 & [\phi_0' \times] \\ O & \frac{d}{dS}\mathbf{1}_3 \end{bmatrix},$$

and

$$\frac{d}{dS}\mathbf{1}_3 := \operatorname{diag}\left[\frac{d}{dS}, \frac{d}{dS}, \frac{d}{dS}\right]. \quad \text{(A2)}$$

Note that we will often use the notation $[\theta \times] \equiv \overset{\vee}{\theta}$.

Tangent Inertia Matrix

The tangent inertia matrix has the following structure:

$$M_{IJ}\left(\Lambda_n, \Lambda_{n+1}^{(i)}\right) = \begin{bmatrix} m_{IJ}^{(1,1)} & O \\ O & m_{IJ}^{(2,2)}\left(\Lambda_n, \Lambda_{n+1}^{(i)}\right) \end{bmatrix} \in \mathbb{R}^{6\times 6}, \quad \text{(A3)}$$

with

$$m_{IJ}^{(1,1)} := \frac{1}{h^2\beta}\left\{\int_{[0,L]} A_\rho N_I(S) N_J(S)\, dS\right\}\mathbf{1}_3, \quad \text{(A4)}$$

$$m_{IJ}^{(2,2)}\left(\Lambda_n, \Lambda_{n+1}^{(i)}\right) := \int_{[0,L]} \left[-\left[\Lambda_{n+1}^{(i)} \left\{ \mathbf{\Pi}_\rho A_{n+1}^{(i)} + W_{n+1}^{(i)} \times \mathbf{\Pi}_\rho W_{n+1}^{(i)} \right\} \times \right] + \frac{1}{h^2\beta} \Lambda_{n+1}^{(i)} \left\{ \mathbf{\Pi}_\rho - h\tau\left[\mathbf{\Pi}_\rho W_{n+1}^{(i)} \times\right] + h\tau\left[W_{n+1}^{(i)} \times\right]\mathbf{\Pi}_\rho \right\} \Lambda_n^T T\left(\theta_{n+1}^{(i)}\right) \right] N_I(S) N_J(S)\, dS, \quad \text{(A5)}$$

with $A = \Lambda^T \alpha$, $W = \Lambda^T W$, and the matrix T defined as follows:

$$T(\theta) := \frac{\theta \otimes \theta}{\|\theta\|^2} + \frac{\|\theta\|/2}{\tan(\|\theta\|/2)}\left[\mathbf{1}_3 - \frac{\theta \otimes \theta}{\|\theta\|^2}\right] - \frac{\overset{\vee}{\theta}}{2}. \quad \text{(A6)}$$

Tangent Material Stiffness Matrix

$$S_{IJ}\left(\phi_{n+1}^{(i)}\right) = \int_{[0,L]} \left\{ \Xi\left(\phi_{n+1}^{(i)}\right)[N_I(S)\mathbf{1}_6] \right\}^T \left\{ c\left(\Lambda_{n+1}^{(i)}\right) \Xi\left(\phi_{n+1}^{(i)}\right)[N_J(S)\mathbf{1}_6] \right\} dS, \quad \text{(A7)}$$

where $c\left(\Lambda_{n+1}^{(i)}\right) := \mathbf{\Pi}\left(\Lambda_{n+1}^{(i)}\right) C \mathbf{\Pi}^T\left(\Lambda_{n+1}^{(i)}\right)$, and $\mathbf{\Pi}(\Lambda) := \operatorname{diag}[\Lambda, \Lambda] \in \mathbb{R}^{6\times 6}$ is a block diagonal matrix.

Tangent Geometric Stiffness Matrix

$$G_{IJ}\left(\phi_{n+1}^{(i)}\right) = \int_{[0,L]} \left\{ \Upsilon[N_I(S)\mathbf{1}_6] \right\}^T \left\{ B\left(\phi_{n+1}^{(i)}\right) \Upsilon[N_J(S)\mathbf{1}_6] \right\} dS, \quad \text{(A8)}$$

where the operator Υ and the matrix B are defined as

$$\Upsilon^T := \begin{bmatrix} \frac{d}{dS}\mathbf{1}_3 & O & O \\ O & \frac{d}{dS}\mathbf{1}_3 & \mathbf{1}_3 \end{bmatrix}, \quad \text{(A9)}$$

$$B(\phi) := \begin{bmatrix} O & O & [-n\times] \\ O & O & [-m\times] \\ [n\times] & O & [n \otimes \phi_O' - (n \cdot \phi_O')\mathbf{1}_3] \end{bmatrix}. \quad \text{(A10)}$$

Tangent Follower Load Stiffness

$$L_{IJ}^a\left(\Lambda_{n+1}^{(i)}\right) = \int_{[0,L]} \begin{bmatrix} O & N_I(S) N_J(S)\left[\bar{n}^a\left(\Lambda_{n+1}^{(i)}\right)\times\right] \\ O & O \end{bmatrix} dS. \quad \text{(A11)}$$

Acknowledgments

This work was performed under the auspices of the Air Force Office of Scientific Research. Partial support for the first author was provided by Grant AFOSR-83-0361 to the University of California, Berkeley. Support for the second author was provided by Grant 2-DJA-544/AFOSR 0292 to Stanford University. These supports as well as the encouragement from Professors K.S. Pister, E. Polak, and R.L. Taylor are gratefully acknowledged.

References

[1] Kline, R.L., "Construction of Large Space Structures," *The Journal of the Astronautical Sciences*, Vol. 27, No. 4, 1979, pp. 401–418.

[2] Canavin, J. R. and Likins, P. W., "Floating Reference Frames for Flexible Spacecraft," *Journal of Spacecraft*, Vol. 14, No. 12, 1977, pp. 724–732.

[3] Benson, D.J. and Hallquist, J.O., "A Simple Rigid Body Algorithm for Structural Dynamics Program," *International Journal of Numerical Methods in Engineering*, Vol. 22, No. 3, 1986, pp. 723–750.

[4] Simo, J.C. and Vu-Quoc, L., "The Role of Nonlinear Theories in Transient Dynamics Analysis of Flexible Structures," Electronics Research Laboratory Memorandum UCB/ERL M86/10, University of California, Berkeley, Jan. 1986. (To appear in *Journal of Sound and Vibration*.)

[5] Simo, J.C. and Vu-Quoc, L., "On The Dynamics of Flexible Beams Under Large Overall Motions—The Plane Case: Part I," *Journal of Applied Mechanics*, Vol. 53, No. 4, 1986, pp. 849–854.

[6] Simo, J.C. and Vu-Quoc, L., "On The Dynamics of Flexible Beams Under Large Overall Motions—The Plane Case: Part II," *Journal of Applied Mechanics*, Vol. 53, No. 4, 1986, pp. 855–863.

[7] Simo, J.C. and Vu-Quoc, L., "On The Dynamics of Finite-Strain Rods Undergoing Large Motions—The Three-Dimensional Case," *Computer Methods in Applied Mechanics and Engineering*, 1987 (to appear).

[8]Simo, J.C. and Vu-Quoc, L., "Three-Dimensional Finite-Strain Rod Model. Part II: Computational Aspects," *Computer Methods in Applied Mechanics and Engineering*, Vol. 58, 1986, pp. 79–116.

[9]Vu-Quoc, L., *Dynamics of Flexible Structures Performing Large Overall Motions: a Geometrically-Nonlinear Approach*, Ph.D. dissertation, Electronics Research Laboratory Memorandum UCB/ERL M86/36, University of California, Berkeley, May 1986.

[10]Newmark, N.M., "A Method of Computation for Structural Dynamics," *ASCE Journal of the Engineering Mechanics Division*, 1959, pp. 67–94.

[11]Hooker, W.W. and Margulies, G., "The Dynamical Attitude Equations for an *n*-Body Satellite," *The Journal of the Astronautical Sciences*, Vol. 12, 1965, pp 123–128.

[12]Roberson, R.E. and Wittenburg, J., "A Dynamical Formalism for an Arbitrary Number of Interconnected Rigid Bodies with Reference to the Problem of Satellite Attitude Control," *Proceedings of the 3rd International Congress on Automatic Control*, Butterworths, London, England, 1967.

[13]Jerkowsky, W., "The Structure of Multibody Dynamic Equations," *Journal of Guidance and Control*, Vol. 1, No. 3, 1978, pp. 173–182.

[14]Huston, R.L., "Multibody Dynamics Including the Effects of Flexibility and Compliance," *Computers & Structures*, Vol. 14, No. 5–6, 1981, pp. 443–451.

[15]Ho, J.Y.L. and Herber, D.R., "Development of Dynamic and Control Simulation of Large Flexible Space Systems," *Journal of Guidance, Control, and Dynamics*, Vol. 8, No. 3, 1985, pp. 374–383.

[16]Hughes, P.C., "Dynamics of a Chain of Flexible Bodies," *The Journal of the Astronautical Sciences*, Vol. 27, 1979, pp. 359–380.

[17]Kane, T.R. and Levinson, D.A., "Multibody Dynamics," *ASME Journal of Applied Mechanics*, Vol. 50, 1983, pp. 1071–1078.

[18]Simo, J.C., "A Finite Strain Beam Formulation. The Three-Dimensional Dynamic Problem. Part I," *Computer Methods in Applied Mechanics and Engineering*, Vol. 49, 1985, pp. 55–70.

[19]Gear, C.W., *Numerical Initial Value Problems in Ordinary Differential Equations*, Prentice-Hall, Englewood Cliffs, NJ, 1971.

[20]Richtmyer, D. and Morton, K.W., *Difference Methods for Initial Value Problems*, 2nd ed., Interscience, NY, 1967.

[21]Belytschko, T. and Hughes, T.J.R., *Computational Methods for Transient Analysis*, Elsevier, 1983.

[22]Goldstein, H., *Classical Mechanics*, 2nd ed., Addison Wesley, Reading, MA, 1980.

[23]Argyris, J.H., "An Excursion into Large Rotations," *Computer Methods in Applied Mechanics and Engineering*, Vol. 32, 1982, pp. 85–155.

[24]Klemperer, W.B. and Baker, R.M.L. Jr., "Satellite Librations," *Astronautica Acta*, Vol. III, fasc. 1, 1957, pp. 16–27.

[25]Roberson, R.E. "Gravitational Torque on a Satellite Vehicle," *Journal of the Franklin Institute*, Vol. 265, 1958, pp. 13–22.

[26]Kane, T.R. and Likins, P.W., "Gravitational Forces and Moments on Spacecraft," NASA CR-2618, Oct. 1975.